REPORT DOCUMENTATION PAGE

Form Approved
OMB No. 0704-0188

1. REPORT DATE *(DD-MM-YYYY)*	**2. REPORT TYPE**	**3. DATES COVERED** *(From - To)*
31-07-2013	Final	01 May 2010 to 30 April 2013

4. TITLE AND SUBTITLE

(YIP 10) Dynamic Silicon Nanophotonics

5a. CONTRACT NUMBER

5b. GRANT NUMBER

FA9550-10-1-0217

5c. PROGRAM ELEMENT NUMBER

6. AUTHOR(S)

Preble, Stefan F.

5d. PROJECT NUMBER

5e. TASK NUMBER

5f. WORK UNIT NUMBER

7. PERFORMING ORGANIZATION NAME(S) AND ADDRESS(ES)

Rochester Institute of Technology
168 Lomb Memorial Dr.
Rochester, NY 14623

8. PERFORMING ORGANIZATION REPORT NUMBER

9. SPONSORING / MONITORING AGENCY NAME(S) AND ADDRESS(ES)

AFOSR
875 North Randolph Street
Suite 325, Room 3112
Arlington, VA 22203

10. SPONSOR/MONITOR'S ACRONYM(S)

AFOSR

11. SPONSOR/MONITOR'S REPORT NUMBER(S)

12. DISTRIBUTION / AVAILABILITY STATEMENT

Approved for public release

13. SUPPLEMENTARY NOTES

14. ABSTRACT

Dynamic tuning of optical cavities enables rich new capabilities that operate with low power, are linear, efficient, compact and CMOS compatible. These dynamic devices are based on the fundamental principle that light propagating within a cavity must inherently match the properties of the cavity at all times. Therefore, when the cavity is dynamically tuned - the lights properties are being directly changed. Consequently, these dynamically tuned silicon nanophotonic devices enable rich new tools for processing optical signals, including, linear wavelength converters, rapidly tunable optical delay devices and robust electro-optic modulators. The following key discoveries were made: (1) Tunable optical delay that enables a >1000x slowing of light in a ~100micron Silicon microring resonator structure; (2) Wavelength conversion at the single photon level by dynamically tuning a microring resonator; (3) Temporal and spectral models of resonators operating in the quantum optical regime; (4) Resonant Hong-Ou-Mandel effect that will enable robust quantum computation and sensing; (5) Robust Phase Shift Keyed Electro-optic Modulators; (6) Efficient micro-oven heater to enhance the thermo-optic tuning of Silicon photonic devices

15. SUBJECT TERMS

Silicon Photonics, Quantum Optics

16. SECURITY CLASSIFICATION OF:			**17. LIMITATION OF ABSTRACT**	**18. NUMBER OF PAGES**	**19a. NAME OF RESPONSIBLE PERSON**
a. REPORT	**b. ABSTRACT**	**c. THIS PAGE**	UU		Stefan F. Preble
U	U	U			**19b. TELEPHONE NUMBER** *(include area code)* 585-475-2625

R·I·T

NANOPHOTONICS GROUP

Young Investigator Program (2010): Dynamic Silicon Nanophotonics

Final Report

Principal Investigator: Professor Stefan Preble
Rochester Institute of Technology
168 Lomb Memorial Dr.
Rochester, NY 14623
585 – 475 – 2625
sfpeen@rit.edu

Award #: AFOSR FA9550-10-1-0217

Program Manager: Dr. Gernot Pomrenke

Performance Period: 1 May 2010 – 30 April 2013

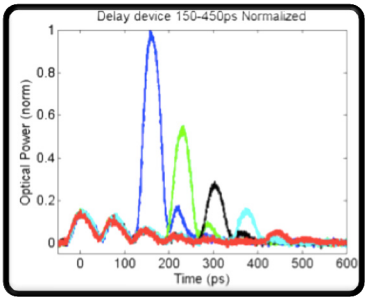

Tunable Optical Delay

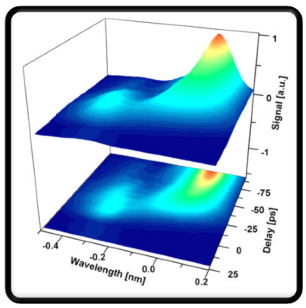

Single Photon Wavelength Conversion

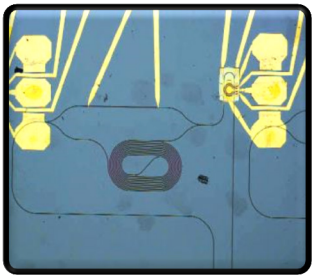

Phase Shift Keyed Modulators

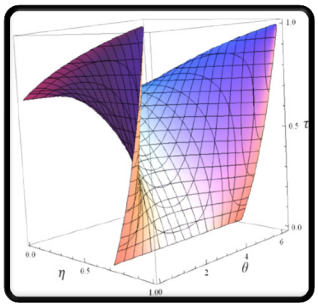

Resonant Hong-Ou-Mandel Effect

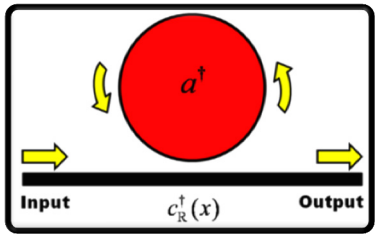

Quantum Optical Resonators

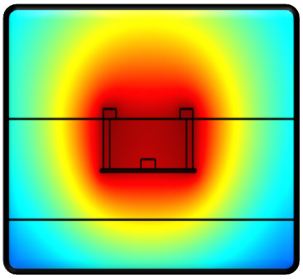

Efficient Micro-oven Heater

TABLE OF CONTENTS

SUMMARY

This final report summarizes the efforts and primary results of the AFOSR Young Investigator Program (YIP) "Dynamic Silicon Nanophotonics" project led by Professor Stefan Preble at the Rochester Institute of Technology. The projects focus is on a new class of nanophotonic devices based on the dynamic tuning of resonant devices. Unlike other approaches dynamic tuning enables rich new capabilities that operate with low power, are linear, efficient, compact and CMOS compatible. These dynamic devices are based on the fundamental principle that light propagating within a cavity must inherently match the properties of the cavity at all times. Therefore, when the cavity is dynamically tuned - the lights properties are being directly changed. Consequently, these dynamically tuned silicon nanophotonic devices enable rich new tools for processing optical signals, including, linear wavelength converters, rapidly tunable optical delay devices and robust electro-optic modulators.

One of the key application spaces for these dynamically controlled devices is where noise must be at a minimum, particularly at the few-photon level, and as a result these devices have significant promise for realizing ultra-secure quantum communication systems and unprecedentedly high performance quantum computation systems. Consequently, a key focus of this project is on the modeling of dynamic photonic devices in the quantum optical regime. However, to do this the resonators and their interactions with arbitrary photon states must be fully understood. Under this program we made the first quantum optical models of resonators and have discovered new phenomena that will be key to realizing robust quantum communication and computing systems based on quantum optical resonator networks.

The following is a summary of the research efforts described throughout the remainder of the report:

Tunable Optical Delay: We have demonstrated a Silicon resonator based optical delay device which traps light for more than 400picosconds in a structure that is only 100microns in size. This is impressive because without the action of the device the light would have travelled nearly 120mm - ~1200x times longer distance. Furthermore, the device can be rapidly reconfigured (>10Gb/s) on demand to realize any arbitrary delay. These properties will prove extremely useful for applications that require such large reconfigurable delays, such as in buffers in computing systems, for feed-forward control in linear quantum optical computation schemes and RF delay lines. Publications: [1-2]

Single Photon Adiabatic Wavelength Conversion: We have demonstrated a new type of wavelength conversion that is purely linear and 100% efficient down to the single photon level. It is achieved by dynamically tuning a microring resonator on a Silicon chip and allows for any arbitrary wavelength change at any time. Through modeling and experimental measurements we proved that adiabatic wavelength conversion operates at the single photon level with no noise and as a result will be key for future quantum optical systems. Publications: [3-4]

Quantum Optical Resonators: We realized the first quantum Finite Difference Time Domain (q-FDTD) simulation model of resonators interacting with photons. The q-FDTD technique was used to understand both adiabatic wavelength conversion and tunable optical delay in the single photon regime. In the future it can be used to model any resonator system in the few-photon regime. Publications: [5-6]

Resonant Hong-Ou-Mandel Effect and Multi-photon Resonator Interactions: We developed a quantum optical model of resonators based on a continuous-wave discrete path integral formalism. A key aspect of this model is that it can be easily applied to understand any resonator network with an arbitrary photon state, including, multi-photon Fock states, coherent and squeezed states of light. One of the key discoveries using this model is that ring resonators exhibit quantum optical resonances that depend on

the photon states themselves. A notable result of this is the manifestation of a resonant Hong-Ou-Mandel effect that could be used to demonstrate linear quantum computation schemes. This would be a significant demonstration as it would enable highly compact and robust quantum optical circuits. In addition, the devices can leverage all of the recent developments in silicon photonics to realize highly reconfigurable and rapidly controlled quantum optical circuits on a Silicon chip. We are collaborating with Dr. Paul Alsing at AFRL/Rome on this work and a theorist supported on this project (Dr. Edwin Hach) joined AFRL during the summers of 2012 & 2013, under the Information Directorates Visiting Faculty Research Program. Publications: [7-8]

Robust Phase Shift Keyed Optical Modulators: We have developed a robust, low insertion loss, compact Silicon ring resonator electro-optic modulator that encodes data in the phase of light, as opposed to amplitude. This has many advantages over amplitude based modulation, including 3dB increase in signal/noise, and reduced nonlinear effects. Our design improves significantly over recently demonstrated PSK modulator designs in terms of insertion loss and stability. We have also experimentally demonstrated the devices robustness by showing that the modulation characteristics are nearly independent of the voltage applied to the modulator. This will be key to future high performance optical interconnect systems. Publications: [9-10]

Micro-Oven Heater: Thermo-optic control is likely to be required in future Silicon photonic circuits in order to counteract fabrication imperfections and temperature variations. We have realized a heater design that doubles heating efficiency over traditional metal resistor heaters and as a result will be critical for these circuits. Our heater effectively forms an “oven” around the Silicon waveguide, strongly confining the heat at the waveguide. Furthermore, the design is fabricated using standard contact’s/via’s in a CMOS process (i.e. that traditionally connect metal layers to silicon transistors) and as a result can be seamlessly integrated in future Silicon photonic circuits. Publications: [11-12]

RESEARCH

Tunable Optical Delay

Tunable delay is a critical component of advanced chipscale optical systems. For example, in communications it will be necessary to delay packets of data in order to reconfigure the communication network. And in quantum optics delay is crucial for realizing feed-forward quantum computing schemes. In the first year of the project we were able to demonstrate a delay device based on a coupled resonant cavity system [1]. Our scheme is continuously tunable, unlike designs based on coupled resonator optical waveguides (CROWs), and can enable very long delays of short pulses of the light. As seen in Fig. 1, the system consists of an input ring resonator (top) which couples the photon into the delay device, a pair of storage resonators (middle) which delay the light, and a release resonator (bottom) which lets the photon leave at any arbitrary time. The device operates as follows: initially the input cavity is tuned to the storage unit cavities to direct the light into the system (Step 1). Next, the state of the input cavity is changed, using free-carriers, to trap the photon in the storage unit (Step 2-3). In order to release the photon from the system, we tune the state of the output cavity to match the storage units (Step 5). Using this approach, a photon can be stored for arbitrary times, only limited by the inherent losses of the waveguides. These losses can be made very low by optimizing the waveguide

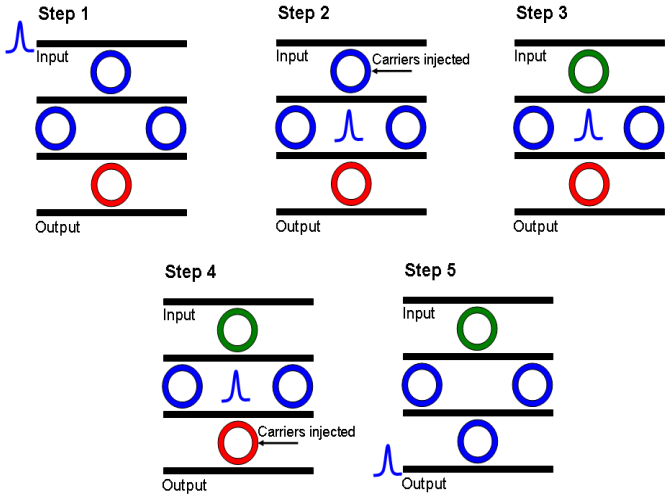

Fig. 1. Schematic of the delay device and its operation principle. The colors of the resonators indicate their state. (Step 1) shows the acceptance state of the system. Photons are stored as

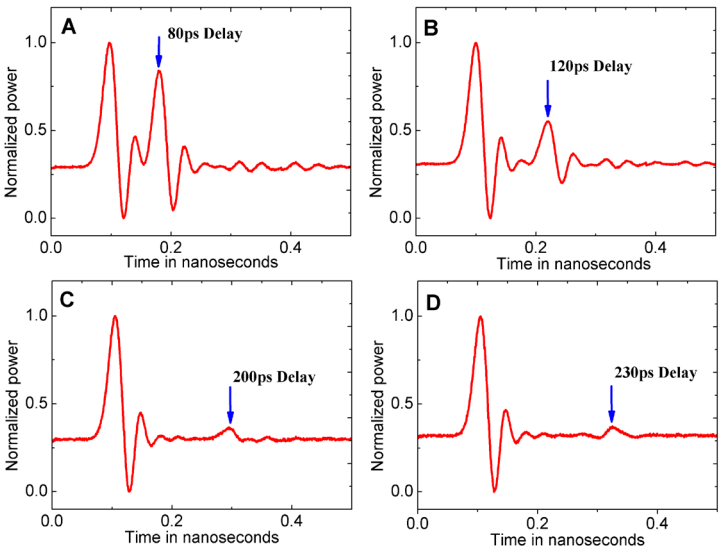

Fig. 2. Different delays are measured by changing the time between the store and the release steps.

fabrication process [26]. In addition, this process is inherently very efficient (>10%) and can be increased to near-unity by incorporating additional resonators to match the state of the system to the photon pulse. Using this we realized ~300ps of delay, as seen in Fig. 2, which was only limited by waveguide loss [1].

In order to improve the waveguide loss we optimized the waveguide geometry [2]. It is well known that the vast majority of loss in silicon waveguides comes from light scattering off the etched sidewalls. To reduce this loss we optimized the waveguide dimensions so that the etch depth is smaller; then we oxidize the waveguides to further reduce the roughness (Fig. 3). We note that it is important to minimize the increase in the device size due to the shallower etch. By realizing a multitude of devices with different etch depths we were able to comprehensively understand this tradeoff .

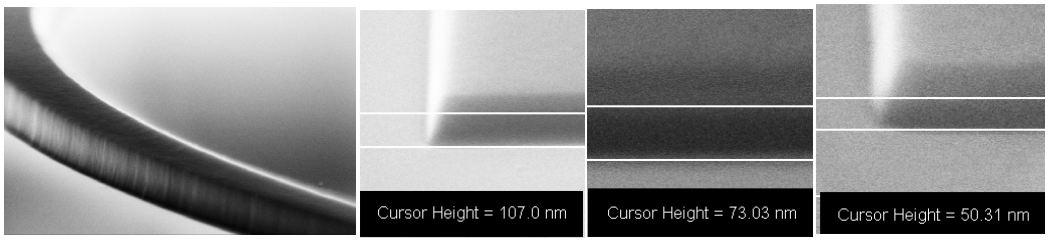

Fig. 3. Typical Silicon waveguide with rough etched sidewalls (left). Reduced loss waveguides with etch depths of 107nm, 73nm and 50nm (right).

Although the most straightforward way to measure waveguide loss is the cut-back method, this is unreliable due to chip facet coupling loss. Therefore to ascertain the waveguide loss we use single-coupled ring resonators with a variety of coupling conditions and sizes, as summarized in the results in Fig. 4 [2]. In the end we found that a 50um radius ring can realize a loaded quality factor of Q=550k which corresponds to an intrinsic Quality factor of Q_{int}=1.6 million, and a waveguide loss of 0.42dB/cm [2]. This is a vast improvement over our previous device with a loss of 8 db/cm and typical silicon waveguides with loss of about 3 db/cm. And using the optimized shallow etch parameters we modeled the proposed delay device using coupled mode theory as shown in Fig. 5, and obtained more than 1nanosecond of delay (of 80ps pulses) with an overall efficiency of greater than 10% [2].

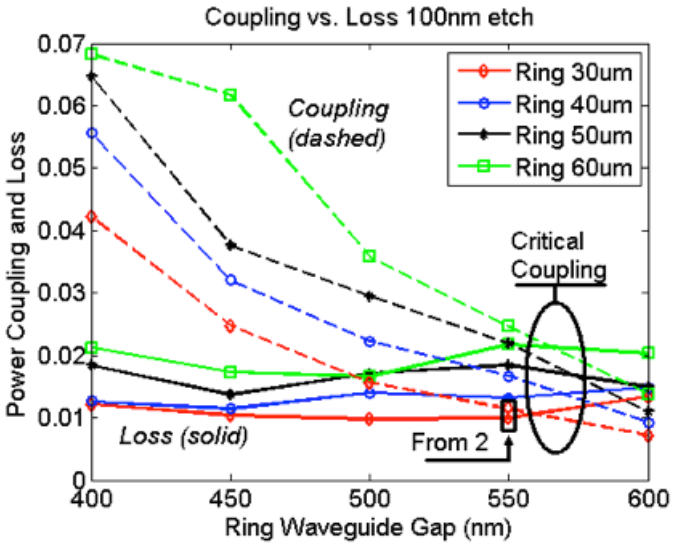

Fig. 4. Analysis of coupling strength and loss in ring resonators with different ring-waveguide gaps. The study is done for rings with multiple radii (30,40,50 and 60um)

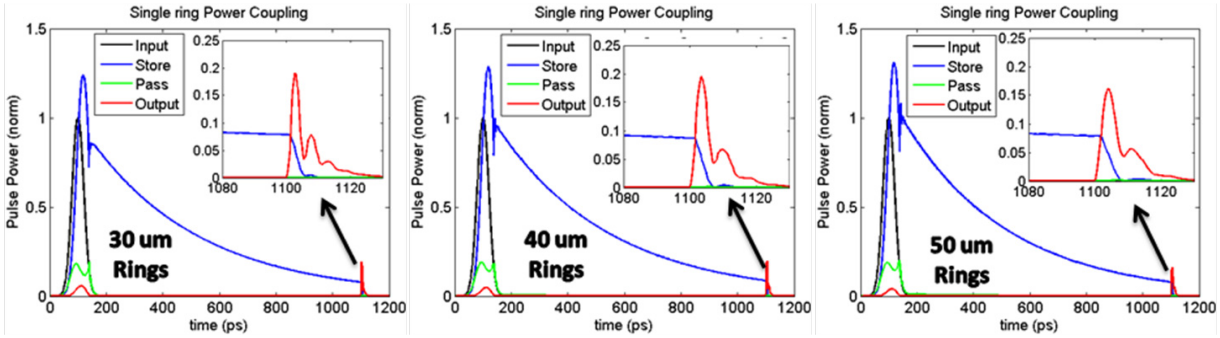

Fig. 5. Simulation of the delay device for different ring resonators. In each an 80ps pulse of light is stored for more than a nanosecond (approximately 300mm of propagation in free-space in only an ~100um structure).

We recently fabricated and characterized the optimized delay device as seen in Fig. 6. **The low loss of the waveguides enabled delay times of greater than 450ps**. However, the delayed signal was attenuated to a level that is equivalent to more than 3dB/cm. As a result we discovered that the delay is no longer limited by waveguide loss but is instead determined by the free-carrier recombination rate. Specifically, the free-carriers recombine too quickly which prematurely couples the stored light back into the input waveguide. This can be overcome through better control of the free-carrier recombination rate, which is controlled by the fabrication process. Or it can be controlled by using electro-optic tuning of the ring resonators, which can use carrier injection/extraction to dictate the dynamics of the carriers as opposed to relying on the inherent characteristics of the material. We are now testing such an electro-optic device and will report/publish the results in the near future.

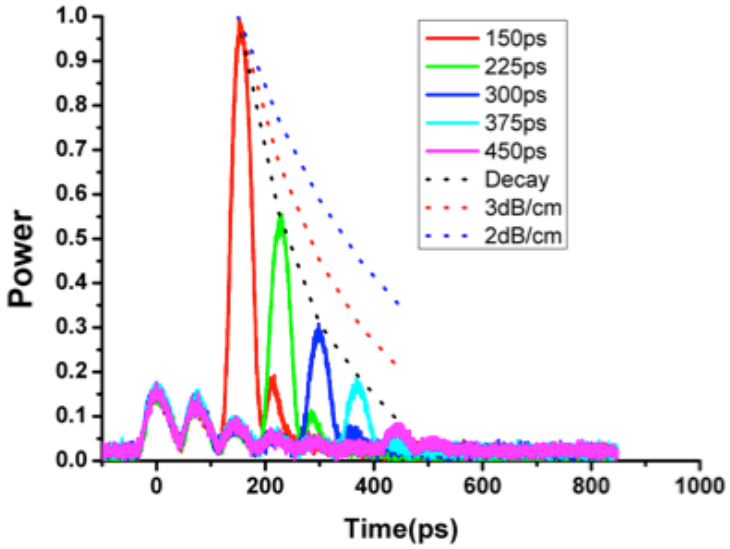

Fig. 6. Measured delay of pulses of light for [150, 225,300, 375 and 450ps]. The decay of the signal exceeds 3dB/cm loss due to free-carrier recombination.

Single Photon Adiabatic Wavelength Conversion

Wavelength conversion is a key requirement for future quantum communication and computing systems, as well as Dense Wavelength Division Multiplexed (DWDM) optical interconnects and telecommunication systems. In 2007 the PI discovered a new type of wavelength conversion, known as adiabatic wavelength conversion, that is 100% efficient – even down to the single photon level [Preble et al, Nature Photonics, 2007]. Furthermore, it is a purely linear effect and as a result does not require phase or energy matching and consequently, high power pump beams. As a result the process is fundamentally noiseless and is ideal for quantum optics applications [3-6].

In this project, as described in the next section "Quantum Optical Resonators", we have proven from fundamental quantum optics principles that adiabatic wavelength conversion is in fact 100%

efficient [6]. Specifically, a photon at one wavelength can have its wavelength changed with complete certainty – provided the photon resides within a resonant cavity while the cavities dielectric properties are being tuned, as described in Fig. 7 [3-6].

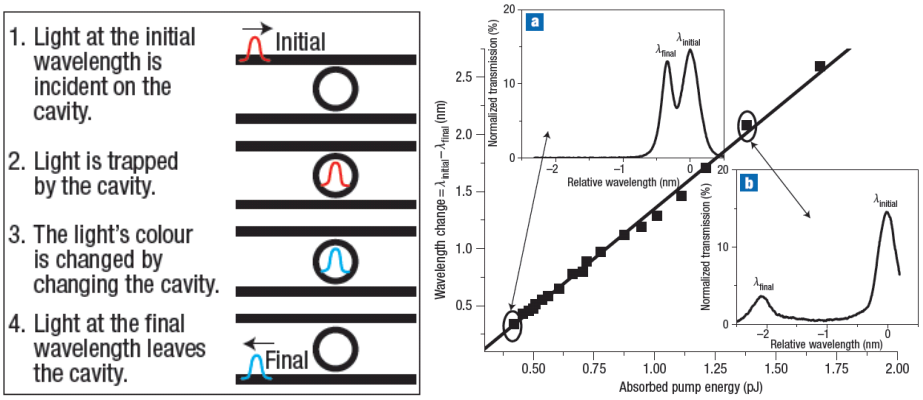

Fig. 7. Adiabatic Wavelength Conversion Process and Results from [Preble, Nature Photonics, 2007]

We have now demonstrated adiabatic wavelength conversion at the single photon level using a Silicon ring resonator and have proven conclusively that is inherently noiseless and as a result a key building block for low noise quantum optics circuits and communication systems [3-4]. It is realized by optically injecting free-carriers into a ring resonator. This is achieved with pump pulses supplied by a Ti:Sapphire laser, as seen in Fig. 8. The laser also pumps an Optical Parametric Oscillator (OPO) to generate the pulses of light at telecommunication wavelengths that will be converted to the new wavelengths. The OPO pulses are filtered at ~1523.2nm (0.14nm bandwidth) and then attenuated to the single photon power level, before being input into the ring resonator. The output of the ring resonator is sent to a switch which allows the response to be either measured by an Optical Spectrum Analyzer (for classical/bright light) or a Single Photon Superconducting Nanowire Detector (SSPD).

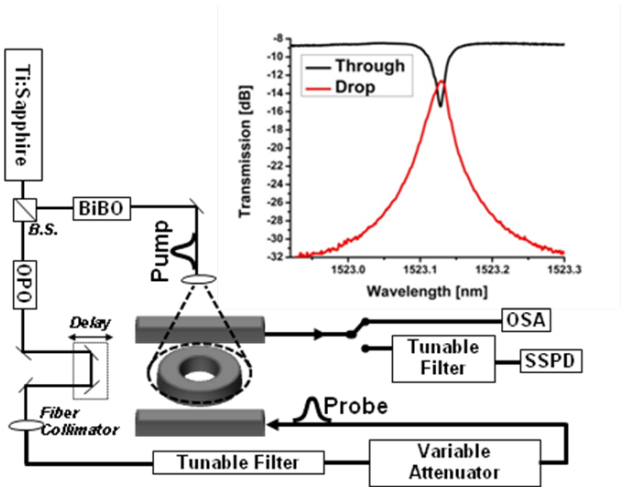

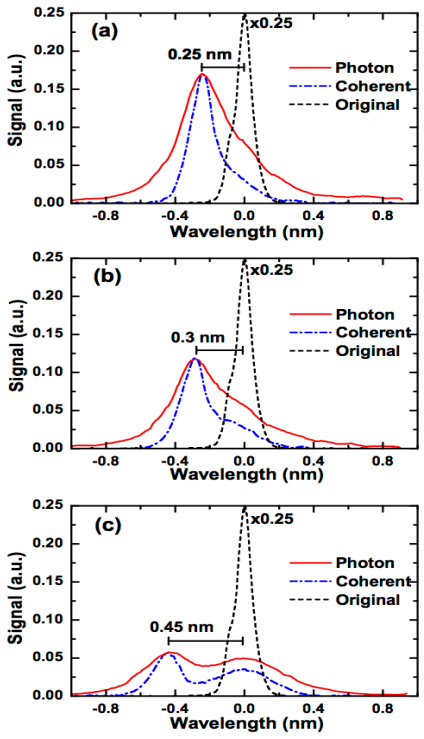

Fig. 8. Experimental setup for single photon adiabatic wavelength conversion. The inset shows the transmission of the Silicon ring resonator. The right figures present the experimental measurements of wavelength conversion to three different wavelengths (a,b,c). The results at the single photon level closely match the results with classical/coherent light, as expected.

Wavelength conversion at the single photon level is seen in the three figures (a,b,c) on the right-side of Fig. 8, which demonstrate wavelength changes of 0.25, 0.3 and 0.45nm, respectively. It is seen that the signal at the single photon power level closely matches the results seen with "classical" (i.e. coherent) light. Importantly, the wavelength change and efficiency is identical to the classical case.

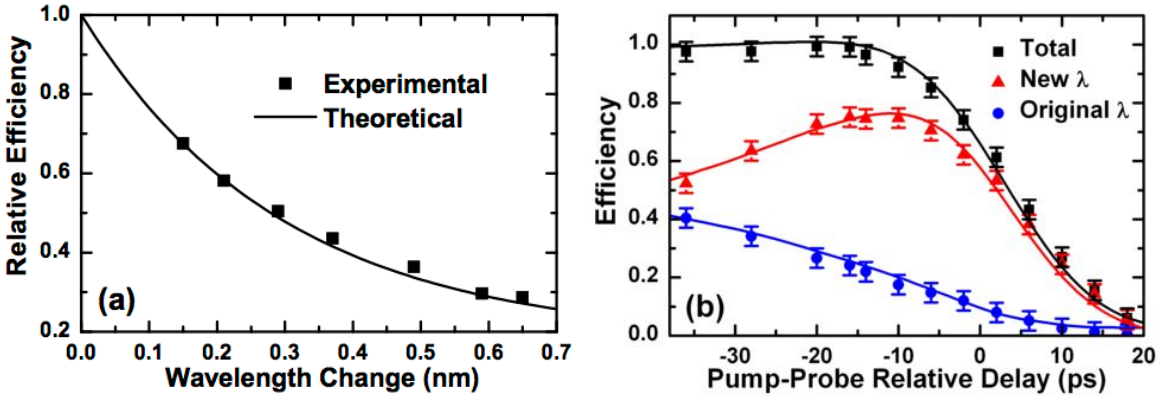

Fig. 9. (a) Free-carrier absorption effect on conversion efficiency **(b)** The photon signals for different pump-probe delays.

A very important consideration for the wavelength conversion process is the conversion efficiency that can be realized. While adiabatic wavelength conversion is inherently 100% efficient there are other loss processes which limit the probability for the photon to exit the resonator at the new wavelength. This is seen in Fig. 9(a) where the relative conversion efficiency exponentially decreases due to free-carrier absorption as the wavelength change is increased [3]. This can be avoided in the future by utilizing tuning mechanisms that do not induce significant absorption effects, such as mechanical tuning. The overall conversion efficiency is also determined by the probability that the photon is within the resonator during the instance the resonator is tuned to its new operating point (i.e. Step 3 in Figure 7). This dependence is seen in Fig. 9(b) where the amount of signal for various pump-probe delays is plotted. Specifically, the wavelength conversion process occurs at a delay of zero and can be considered to occur near-instantaneously since the pump pulse is relatively short (<200fs). If the photon is converted too soon (t > 0) then the pulse won't couple into the cavity. And if the light is converted too late (t<<0) the pulse will have already left the cavity. Consequently, optimal conversion is achieved when most of the pulse is within the cavity. For our photon pulse duration (~10ps) this yields an 80% conversion efficiency when neglecting free-carrier absorption effects [3]. The exact peak efficiency can of course be optimized by closely matching the pulses duration to the photon lifetime of the cavity.

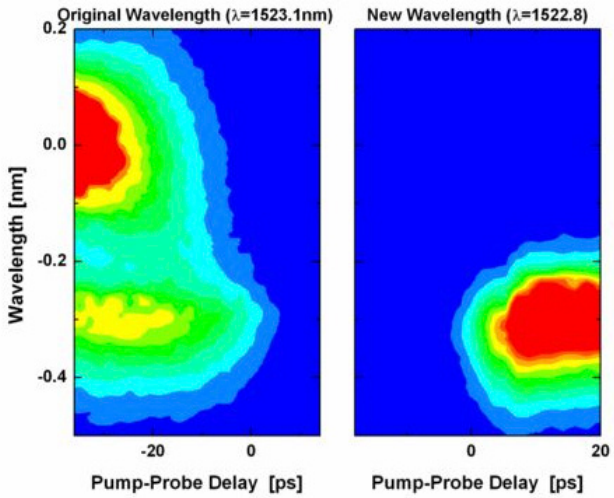

Fig. 10. Spectrum of the photon for different pump-probe delays. Left panel is when the photon begins at the original wavelength. Right is when it is tuned to the new wavelength.

Lastly, we see in Fig 10 the photons spectrum for different pump-probe delays. In the left panel light at the original wavelength (1523.1nm) is converted to a new wavelength $\Delta\lambda$=-0.3nm away. In addition it is seen that at pump-probe delays near t~0 that all of the photon has been converted to the new wavelength and none remains at the original wavelength, as expected since adiabatic wavelength conversion is 100% efficient. This is further proven in the right panel which shows that if the photon has a wavelength that is tuned to the cavities *new* state then there is only a signal for t>0, as expected, since photons at this wavelength would only be transmitted past the ring resonator in Fig. 8 once the resonator is on-resonance with the wavelength. **Consequently, we have proven that adiabatic wavelength conversion is fundamentally noiseless and as a result is a key functionality for future quantum optical computation and communication systems.**

Quantum Optical Resonators

We have been investigating the quantum optical interaction of photons with ring resonators [5-8]. We initially developed a fully quantum mechanical model to describe both the frequency and time-dynamics of single photons interacting with a cavity. From these results we modeled single photon adiabatic wavelength conversion and single photon optical delay as described here. We have now extended this work to multi-photon resonator interactions as described in the next section on "Resonant Hong-Ou-Mandel Effect".

Quantum information science has shown that quantum mechanical effects can revolutionize the performance of communication, computational and measurement systems. And one of the most promising approaches to realizing quantum mechanical effects is with "quantum optics," because photons can be easily manipulated using standard optical components and they are inherently immune to decoherence effects. Quantum optics has already proven to have enormous promise for revolutionary new technologies, such as fundamentally secure communication, measurement precision beyond the standard quantum limit, and the ability to beat the diffraction limit. And one of the most intriguing and potentially breakthrough technologies is quantum computation, which would out-perform classical computers on certain problems by orders of magnitude. However, until recently quantum optics demonstrations have relied on bulk optical elements (lenses, mirrors, beam splitters, etc.) attached to a large table - greatly limiting their performance and scalability. It is now clear that chip-scale integration is fundamental to the realization of a quantum optical computer. In particular, one of the most promising approaches to quantum computation is known as Linear Optical Quantum Computing (LOQC). It only requires linear optical elements (such as directional couplers and phase shifters) and single photon detectors to induce a

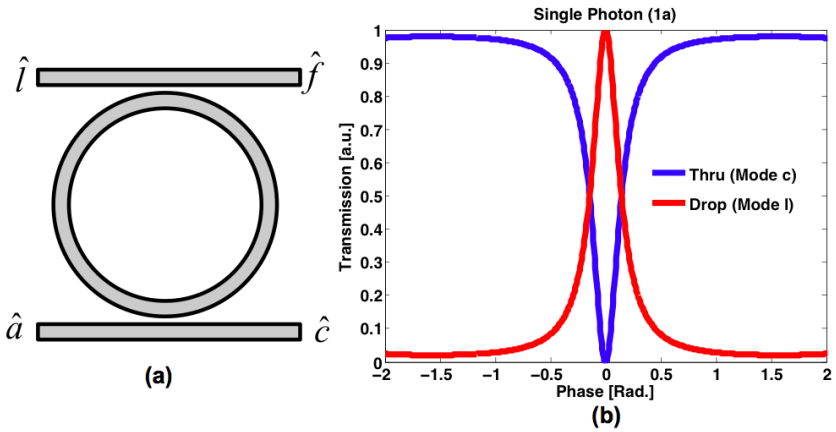

Fig. 11. (a) Ring resonator coupled to two waveguides. (b) Calculated single photon transmission of the ring resonator. The photon is incident on mode a and is either transmitted to thru port (mode c) or the drop port (mode l).

measurement based 'non-linearity' which yields the computation result [Knill, Laflamme and Milburn, Nature 409, 2001]. However, the most significant challenge of LOQC is that it is inherently non-deterministic. Knill, Laflamme and Milburn (KLM) showed that this is not a fundamental limitation, but there is still considerable progress that must be made in device performance and integration in order to realize error-free quantum computation. Silicon photonics is an ideal solution because it will allow the integration of all of the necessary photon sources, detectors, and quantum circuits.

It can be argued that a lot of the success of silicon photonics platform is due to the resonator, which enables compact, high performance devices that can be used as a building block for a multitude of functionalities from electro-optic modulation to photon generation. Similarly we will show here and in the next section the ring resonators are going to be a key building block for future quantum optical circuits. A schematic of a single ring resonator coupled to two waveguides is seen in Fig. 11(a). We have previously modeled the response of a ring resonator to a single photon as seen in Fig. 11(b) using a fully quantum-mechanical approach [6]. While the resonance response, as expected, is similar to the result one would obtain using classical models, it is important to note that the interpretation of the resonance is very different since it is the result of single photon interference.

Using our quantum mechanical resonator model we were able to realize a quantum optical finite-difference-time-domain (q-FDTD) simulation of a ring resonator. We see in Fig. 12 that as a photon propagates in space-time and is coupled to a cavity it becomes split in both space-time [6]. The larger peak of the wavefunction is due to light that is not coupled into the resonator. The smaller peak is due to light that is coupled into the resonator and then leaks back out. Consequently, there is inherently a space-time correlation induced by a cavity. This is equivalent to path entanglement where a photon is split by a beam splitter – but here it is realized in time. Furthermore, by tuning the cavities properties it is possible to tailor this cavity-waveguide entanglement.

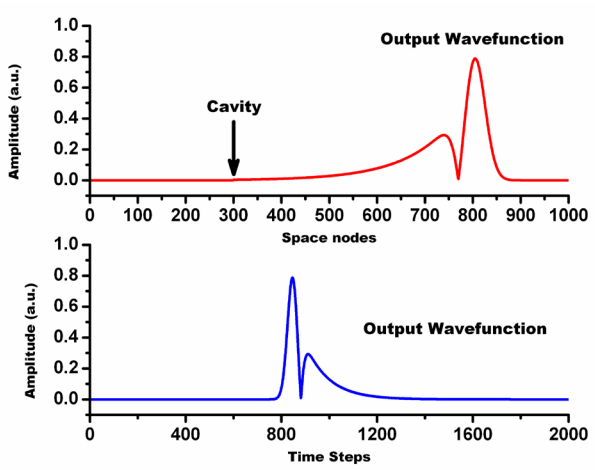

Fig. 12. Space and time profile of a single photon coupled to a ring resonator cavity.

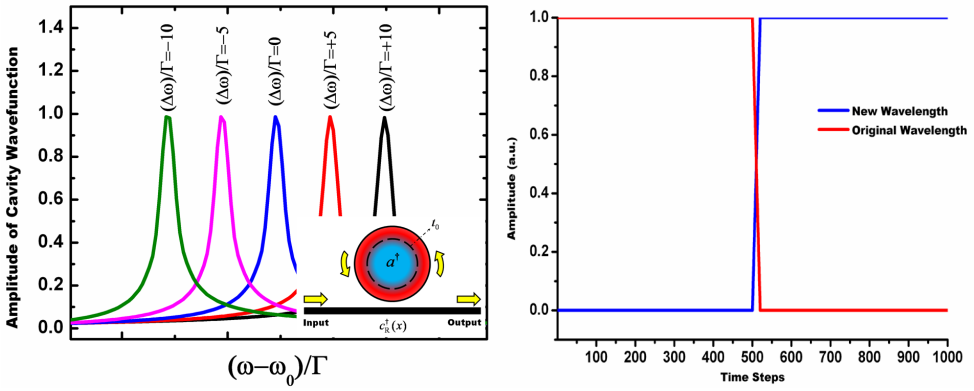

Fig. 13. Spectrum of photon converted to different frequencies through adiabatic tuning of the cavity (inset). The right figure shows that the photon is converted completely to a new wavelength.

Our q-FDTD was also applied to understanding adiabatic wavelength conversion and tunable optical delay. In Fig. 13 a cavities eigenstate is dynamically tuned from an initial resonant frequency to a new frequency once the photon pulse enters the cavity. As seen in the spectrum in the figure all of the photons frequency can be changed to any arbitrary new frequency. Furthermore, the right graph shows that all of the photon at the original frequency has been converted to the new frequency once the frequency conversion process is completed at t~500. Consequently, our quantum optical model proves that adiabatic wavelength conversion is 100% efficient and noiseless [6]. Furthermore, as seen in Fig. 14 the q-FDTD model can be directly applied to complex systems of cavities, such as the tunable delay discussed earlier [6].

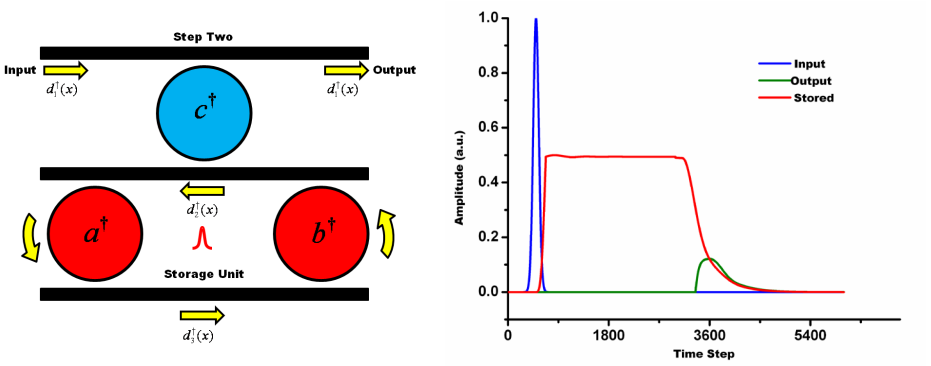

Fig. 14. Storage of single photons in the tunable delay device.

Resonant Hong-Ou-Mandel Effect (Collaboration with AFRL Rome)

Here we present an entirely new class of quantum photonic resonators that exhibit non-classical photon interference. In addition, we have found that the quantum interference is considerably more robust than non-resonant counterparts (such as directional couplers and Mach-Zehnders). This will directly lead to an entirely new type of quantum circuits that are built from resonant quantum optical gates that are robust, can be reconfigured with ultra-lower energies (<100fJ/bit), switched at high speeds (>GHz) and are compact (<2micron). This would directly enable robust and high performance active control of qubits, which is key to achieving deterministic quantum computation.

In order to analyze the response of resonators to multiple photons we have developed a new discrete path integral approach that can be used to arrive at quantum mechanical linear transformations relating the Boson operators along the output modes of a resonator (or any network of linear optical elements) to those along the input modes [7-8]. For the case of the ring resonator shown in Fig. 15 this can be derived to be:

$$\begin{pmatrix}\hat{c}\\ \hat{l}\end{pmatrix}=\begin{pmatrix}t & s'\\ s & t'\end{pmatrix}\begin{pmatrix}\hat{a}\\ \hat{f}\end{pmatrix}\Rightarrow\begin{pmatrix}\hat{a}\\ \hat{f}\end{pmatrix}=\begin{pmatrix}t^* & s^*\\ s'^* & t'^*\end{pmatrix}\begin{pmatrix}\hat{c}\\ \hat{l}\end{pmatrix}\Rightarrow\begin{pmatrix}\hat{a}^\dagger\\ \hat{f}^\dagger\end{pmatrix}=\begin{pmatrix}t & s\\ s' & t'\end{pmatrix}\begin{pmatrix}\hat{c}^\dagger\\ \hat{l}^\dagger\end{pmatrix}. \quad (1)$$

For convenience, we have defined the transition amplitudes

$$t\equiv\left(\frac{\eta^*-\tau e^{i\theta}}{\eta^*\tau^*-e^{i\theta}}\right),\ s\equiv\left(\frac{\gamma\kappa^* e^{i\phi_2}}{\eta^*\tau^*-e^{i\theta}}\right);\ t'\equiv\left(\frac{\tau^*-\eta e^{i\theta}}{\eta^*\tau^*-e^{i\theta}}\right),\ s'\equiv\left(\frac{\kappa\gamma^* e^{i\phi_1}}{\eta^*\tau^*-e^{i\theta}}\right) \quad (2)$$

using which it is straightforward to verify that Bosonic commutation relations are satisfied in the output mode operators. The form of this linear transformation is anticipated. Indeed, proceeding to the

parametric limit this result reduces to the corresponding classical result presented some years ago by Yariv [A. Yariv, Electronics Letters 36, 321 (2000)].

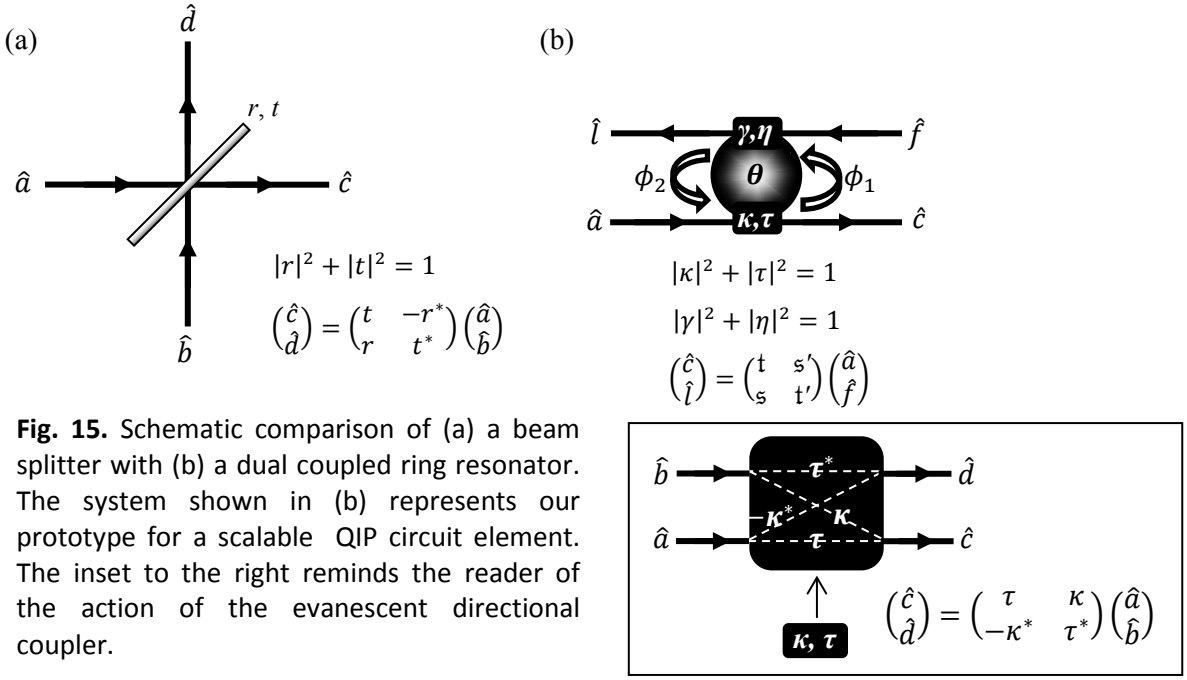

Fig. 15. Schematic comparison of (a) a beam splitter with (b) a dual coupled ring resonator. The system shown in (b) represents our prototype for a scalable QIP circuit element. The inset to the right reminds the reader of the action of the evanescent directional coupler.

The implications of the response of a ring resonator to multiple photons is most clearly elucidated in the case where two photons are input into the resonator simultaneously from two separate inputs, along modes â and f̂, $|\psi_{in}\rangle = \hat{a}^\dagger\hat{f}^\dagger|\emptyset\rangle = |1,1\rangle$. In the output modes we find $|\psi_{out}\rangle = \sqrt{2}ts'|2,0\rangle + (ss' + tt')|1,1\rangle + \sqrt{2}t's|0,2\rangle$. It is clear upon inspection of this result that when $ss' + tt' = 0$ is satisfied then $(1,1) = |ss' + tt'|^2$ vanishes. Or in other words, the photons will bunch together, either into output mode ĉ or $\hat{l}$ with equal probability. This is similar to the well-known Hong-Ou-Mandel (HOM) effect observed in 50/50 beam splitters and is of unparalleled importance to linear quantum optical computation (LQOC) , such as the KLM computation protocol, since it forms the basis for all universal quantum logic gates.

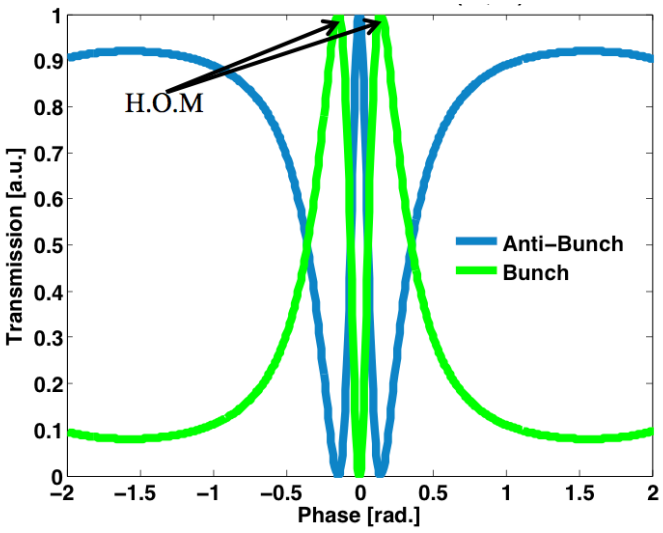

Fig. 16. Two photon interference in a ring resonator. The photons phase (frequency/wavelength) determines whether the photons will Bunch (both go to output c or both go to output l – also known as the Hong-Ou-Mandel [H.O.M] effect) or Anti-Bunch (they split apart).

However, unlike the case in a beam splitter, the HOM effect in ring resonators is resonant as seen in Fig. 16. First we note that this response is markedly different from the classical/single photon case

presented in Fig. 11 and shows for the first time that resonators operating in quantum optical regimes operate fundamentally differently. Secondly, unlike a 50/50 beam splitter, there are an **infinite** number of conditions where HOM resonance is realized. Specifically, the H-O-M Effect is obtained as long as the constraint ss'+tt'=0 is satisfied, which we refer to as a strong form of the Hong-Ou-Mandel Manifold Constraint (sHOMMC).

To appreciate the importance of the sHOMMC, consider the parameter space of the device pictured in Fig. (15b) in comparison with that of an ordinary, lossless beam splitter as in Fig. (15a). In the former case, the four complex parameters κ, τ, γ, and η, along with the single real parameter θ characterize a nine dimensional manifold that is the parameter space of the system. Of these nine dimensions, the four phases of the coupling parameters are essentially redundant. In practice, these phases are typically determined by the details of the construction of the coupler and thusly do not represent truly "free" parameters within the operating space of the device. In any case, these phases can be adjusted either on-chip or in bulk optics via linear phase shifters. For analogous reasons, the general operation of a beam splitter can be described without loss of generality using a one dimensional parameter space, the H-O-M Effect occurring for an individual (50/50) operating point (i.e. a zero dimensional "Hong-Ou-Mandel Manifold") within that one dimensional parameter space. As we now examine, the sHOMMC establishes the existence of higher (>0) dimensional manifolds that are level sets of operating points for which the device shown in Fig. (15b) exhibits the H-O-M Effect.

To clarify the result we examine case in which the device shown in Fig. (15b) is characterized via $\tau = \eta \in \mathbb{R}$ and $\kappa = \gamma = ik, k = \sqrt{1-\tau^2} \in \mathbb{R}$. We note that these constraints, while restrictive, are experimentally relevant to all of the ring resonators we have presented in this report. This constraint corresponds at exact resonance with the optical balance condition for critical coupling. In this case, the parameter space of the device is restricted to two dimensions. Here we take the free parameters to be τ and θ. Applying these constraints to the sHOMMC and using Eqn. (2), we plot in Figure (17) the probability of output photon coincidence in modes l and c versus the free parameters of the system. It is precisely the bottom of the "valley of zeroes" of the $P(1,1)$ that is the one dimensional HOMM for this system. In obvious contrast to the 50/50 beam splitter, which has a single H-O-M operating point, the system shown in Fig. (15b) has, in this case, infinitely many such operating points. This level set of vanishing probability for photon coincidence is the one dimensional HOMM within the two dimensional parameter space of the system in this case.

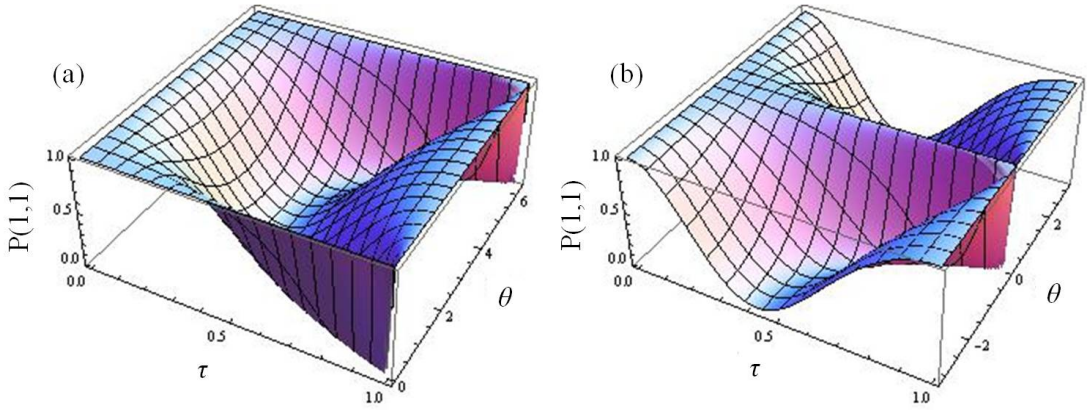

Fig. 17. Surface plot of the probability, P(1,1), for output photon coincidence for the case in which two incident photons are coincident on the ring along modes a and f. The Hong-Ou-Mandel Effect are the zeroes of this surface plot.

The level set of zeroes forms a continuous manifold in this case; it is a one dimensional Hong-Ou-Mandel Manifold (HOMM). We display the same result over the ranges (a) $\theta \in [0,2\pi]$ and (b) $\theta \in [-\pi,\pi]$. We do this merely for ease of visualization and reference; the two plots in each figure so displayed convey exactly the same information.

The broader importance of the results we have presented here is really two-fold. First, we have demonstrated that a ring resonator evanescently coupled to two waveguides as shown in Fig. (15b) is a system capable of "routing" input photons in accordance with the well-known Hong-Ou-Mandel Effect. Unlike the situation in bulk optics; however, the system we have analyzed here is scalable and can be fabricated in large numbers. These attributes suggest that such system could be easily engineered for on-chip implementation of the H-O-M Effect, a staple of many, if not all, quantum information processing architectures based upon linear quantum optics.

Second, we have demonstrated that the range of parameters for which the ring resonator system demonstrates H-O-M behavior is infinitely larger than the corresponding range in the typical beam splitter version of the effect. This fact, combined with the dynamical tunability of the waveguide/ring resonator coupling allows for the possibility of robust photon "routing" unlike that possible with a beam splitter. In this sense, the H-O-M Effect is more robust in the ring resonator set-up than it is in its beam splitter implementation. What we have demonstrated here is that, by virtue of the existence of the sHOMMc within the parameter space of the waveguide/ring resonator system, we can produce on-chip, scalable, robust quantum optical interconnects for integration into photonic quantum information devices. We have already designed a Nonlinear Sign (NS) gate which we will publish on in the near future.

Robust Phase Shift Keyed Optical Modulators

The fundamental element of any optical interconnect is the electro-optic modulator, and there have been many successful demonstrations of amplitude based silicon modulators. However, phase encoded modulation has been required for the advancement of all communication technologies. For example, while amplitude modulation was used in optical fiber communications for decades, by the beginning of the last decade there was a rapid transition to phase based encodings due to the exponentially increasing bandwidth requirements of the internet. Silicon photonics is experiencing a similar demand for bandwidth and will also need to move towards using phase encodings. There are several reasons that phase modulation is preferred over amplitude modulation: (1) Maximization of signal/noise (SNR); (2) Minimization of nonlinear effects; (3) Maximization of channel efficiency (which translates to increased system bandwidth).

There have been several recent investigations of using ring resonators to generate phase-encoded signals [10]. However, they all suffer from high insertion loss – resulting in no SNR enhancement over amplitude based modulation formats. Here we have realized a novel design that breaks the limitations of current ring based PSK modulators. First, to understand our design consider a single-coupler ring resonator (Single Coupler in the slide) operating in an over-coupled state, Fig. 18 (left). By modulating around the resonant wavelength, a pi phase shift can be achieved, with relatively equal amplitudes. However, these amplitudes are significantly less than 1, or in other words there is a high insertion loss. Furthermore, this approach requires precise modulation voltages otherwise non-ideal phase changes will be obtained.

To overcome these issues we have proposed to use a dual-coupler ring resonator, Fig. 18 (middle) and switch between an on-resonance (pi phase shift) and off-resonance (0 phase shift)

condition. With a traditional dual-coupled design the 0 and pi phase modulations will be output on separate waveguides. To correct this we combine the output Y1 to the input X2, which we call a feed-through dual coupled ring, Fig. 18 (right). This design not only gives the required 0 to pi phase changes over a large portion of the spectrum, with negligible insertion loss, but also allows for fine tuning of this phase difference in the feed-through arm. This design is highly robust against fabrication imperfections and variances in the modulating voltage.

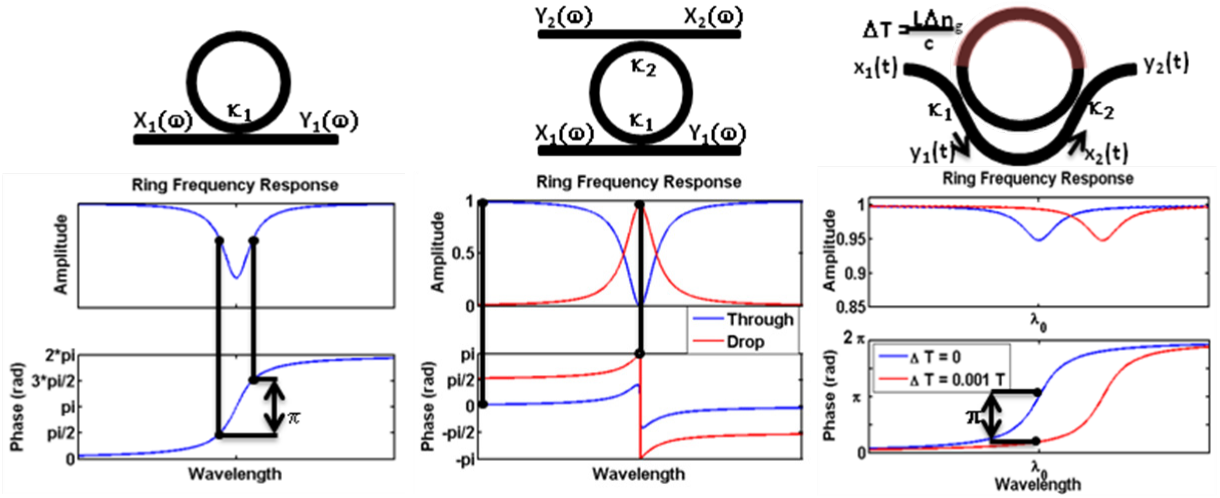

Fig. 18. (left) Over-coupled ring resonator used for PSK with two near-resonance operating points. (middle) Dual-coupler ring resonator (right) Proposed feed-through PSK modulator ring resonator

To further model the PSK device performance we simulated the response of a forward biased PIN junction waveguide (Fig. 19). This will inject carriers (both electrons and holes) into the waveguide, and by the free-carrier-plasma-dispersion effect the refractive index (and loss) will be changed. As we see on the right due to the sharp turn-on of the PN junction, we have a sharp phase response of our device as a function of input voltage. This characteristic makes the modulator robust to voltage variation, as seen in the Fig. 19(d). Specifically, the pi (-180 degree) and 0 phase responses are realized over a wide-range of voltages.

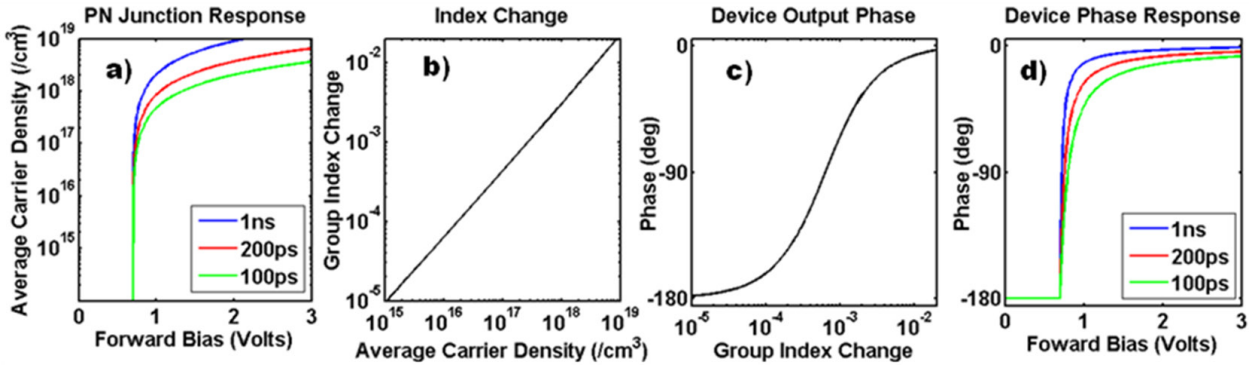

Fig. 19. (a) Carrier density for different voltages and response times in a PIN modulator. (b) Index change for different carrier densities. (c) Output phase change for PSK modulator for different index changes. (d) Overall PSK phase response for various voltages.

In order to demonstrate the high speed response of the PSK modulator we start with voltage modulations at 10 Gbps with voltages of 1-4Vpp using both square and sine wave inputs (Fig. 20a). This leads to a variety of carrier responses, but the phase output (Fig. 20d) remains relatively constant for all of these modulations. Even better, the output of a differential phase shift keyed (DPSK) detector (used commonly in most PSK systems) shows even less variation as seen in Fig. 20e. **Therefore we can conclude that our device is robust against modulation variation** [10]**.** This is confirmed in Fig. 21 which shows the experimentally measured modulation of a fabricated PSK electro-optic modulator for a variety of voltages. It is seen that the modulation output is independent of voltage [9].

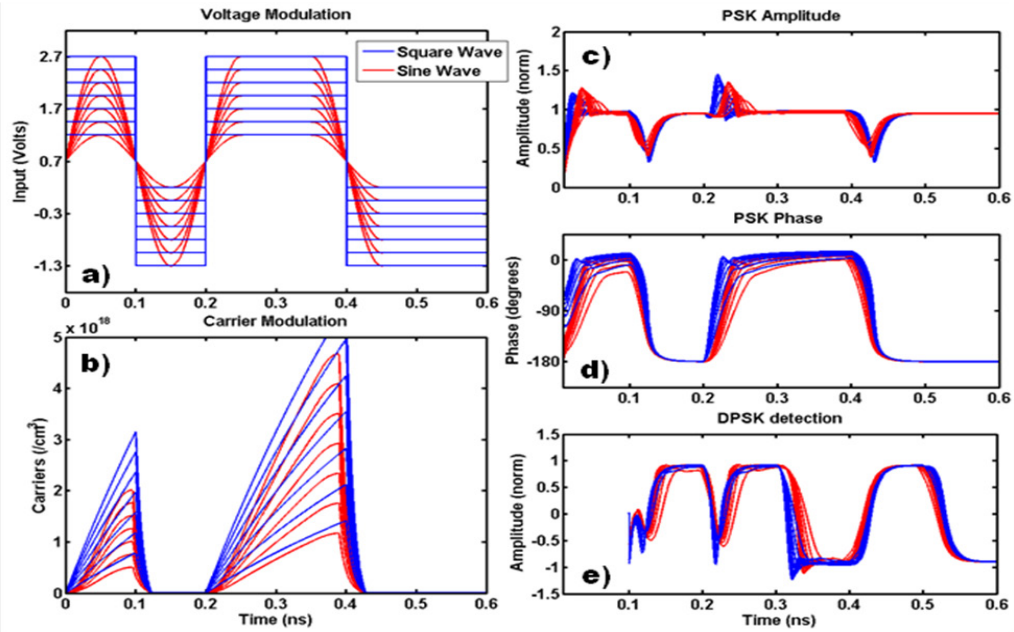

Fig. 20. a) Modulating voltage input (50-200% of optimal) with square wave and sine wave (~100ps rise) signals. b) Average carrier concentration in the waveguide. c) Optical output amplitude and d) optical output phase of the proposed device. e) Signal amplitude resulting from differential detection. Levels yield a 2.5db ± 0.2db output.

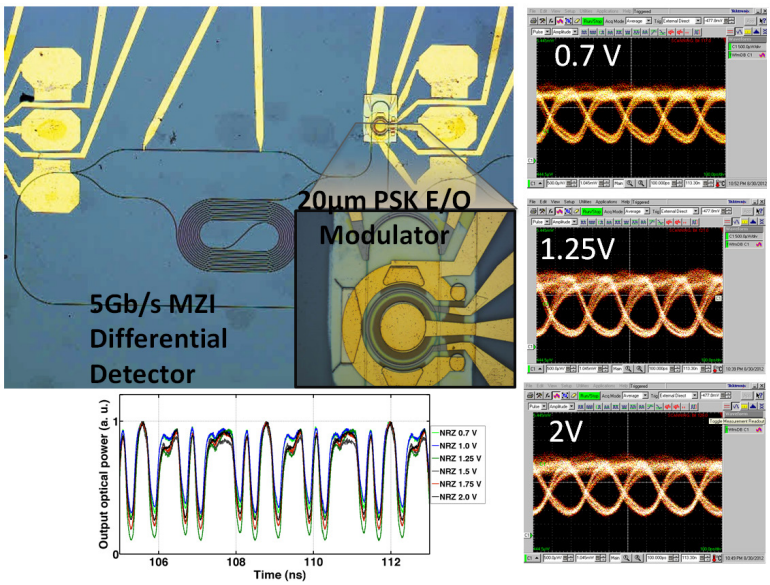

Fig. 21. Experimentally measured PSK modulation for a variety of voltages. The left-upper figure shows a microscope image of the PSK E/O modulator and an integrated one-bit delayed Mach-Zehnder Interferometer differential detector. The bottom graph shows a portion of the modulation output for a wide range of modulation voltages. The right graphs show open eye-diagrams for three different applied voltages [0.7V,1.25V and 2V].

Micro-oven Heater

Silicon photonics is one of the most promising platforms for board level and chip level interconnects due to its broadband, high speed, and low power operation. One of the key building blocks for Silicon photonic interconnects is the electro-optic modulator. The most efficient modulator designs are based on either ring or disc resonator structures. However, these compact ring or disc structures are sensitive to fabrication imperfections and small temperature changes, therefore they are challenging to integrate into high yield mass production that is key to realizing complex optoelectronic interconnects. The simplest and most traditional way to introduce thermal control is with a high resistance metal resistor on top of the cladding oxide, as seen in Fig. 22(a). The current through the resistor will induce Joule heating which will gradually transfer to the silicon waveguide and therefore change the performance of the resonator. However, due to the poor thermal conductivity of the cladding oxide, the efficiency of this method is very low. This can be mitigated slightly by using a thinner cladding oxide but this has a tradeoff of additional optical loss. Here we present a new Silicon photonic heater based on a micro-oven structure in order to enhance heating efficiency of silicon photonic devices [11-12]. The micro-oven is seamlessly integrated in a CMOS photonic fabrication flow since it does not require additional process steps or even materials. It directly makes use of the standard metal contacts/via's used to connect upper Metal layers to the active Silicon devices. Furthermore, the metal contacts effectively form an "oven" around the Silicon waveguide, in turn, confining the thermal energy.

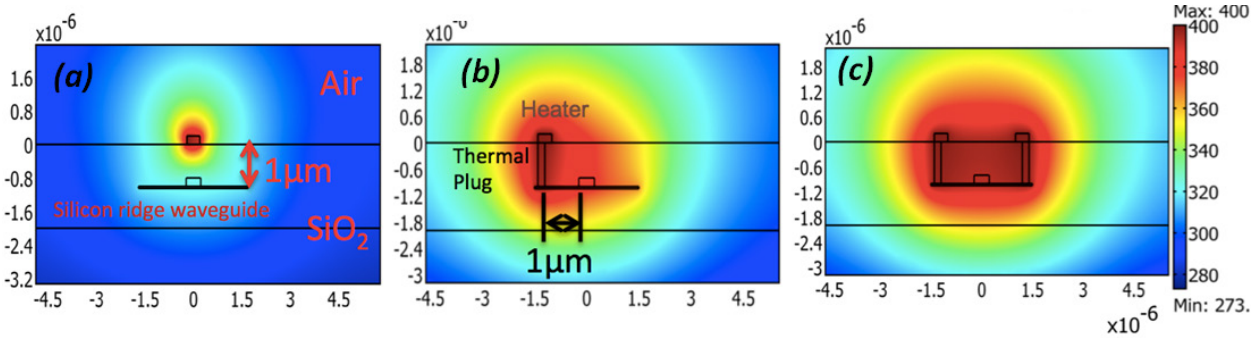

Fig. 22. FEM simulations of heating of a (a) Traditional top heater; (b) Thermal contact on one side of the waveguide; (c) Micro-oven heater

The traditional approach for achieving thermal control is with a high resistivity metal. To avoid optical loss the resistor is normally separated from the silicon waveguide by a thick cladding oxide (>1 micron). Unfortunately, the poor thermal conductivity of silicon oxide (k=1Wm-1K-1) results in a low thermal efficiency (34.1%), defined as the temperature of the Silicon waveguide relative to the temperature of the heater, as seen in the 2D Finite-Element-Method (FEM) simulation in Fig. 22a. In a modified approach, we channel heat to the slab region of the silicon waveguide without affecting the optical mode by using a high thermal con ductivity metal contact (k=400 Wm-1k-1), such as Copper, placed 1micron away from the Silicon waveguide. Furthermore, since the Silicon slab has a much higher thermal conductivity (149Wm-1k-1) than oxide the heat is transferred relatively efficiently (82.6%), to the Silicon waveguide, as seen in Fig. 22b. To enhance the thermal efficiency further we add an identical thermal metal contact at the other side of the waveguide. This strongly confines the thermal energy in the central region as seen in Fig. 22c. As a result we achieve a very high efficiency of 94%. We have named this heater design a "micro-oven" due to the similarity to any oven used in a kitchen (i.e. an oven consists of high thermal conductivity walls surrounding a low thermal conductivity region). Specifically, the device efficiently conducts and confines heat through the low thermal resistivity thermal contacts that completely surround the central waveguide region.

To prove the micro-oven concept experimentally ring resonators were fabricated with either the traditional or micro-oven heater. The fabrication starts from 250nm thick Silicon on a SOI wafer with a 3micron of buffer oxide. Waveguides with a width of 450nm are patterned with HSQ resist by electron beam lithography. After developing, the unprotected area is etched down by 200nm by reactive ion etching under inductively coupled plasma (ICP) chlorine chemistry, leaving 50nm silicon slab next to the waveguide. Then 1.5 micron of PECVD Oxide is deposited over the waveguide as a cladding; and 80nm thick NiCr is patterned over the ring resonator region with width of 1.5micron as the heater source. The traditional heater configuration is then formed. After that, thermal contact holes are patterned and etched 1.5micron away from the silicon waveguide, Aluminum is then deposited and lifted-off to fill the contact holes to serve as the thermal conductor and micro-oven chamber. And finally 50nm of gold is patterned as the contact pads for both types of heaters.

The measured spectral response of a 2.5micron radius ring resonator with a micro-oven heater under different heating powers is seen in Fig. 23a. The spectral behaviors of 2.5micron radius devices with traditional heater design and double ring oven design is also extracted in Fig. 23b for comparison. We see that both micro-oven heater designs exhibit a wavelength shift of ~0.8nm/mW while the traditional heater has a wavelength shift of only 0.35nm/mW. Consequently, we see that the micro-oven doubles the heater efficiency [11]. Further improvements in the fabrication process are expected to yield even higher efficiencies as predicted by the simulations.

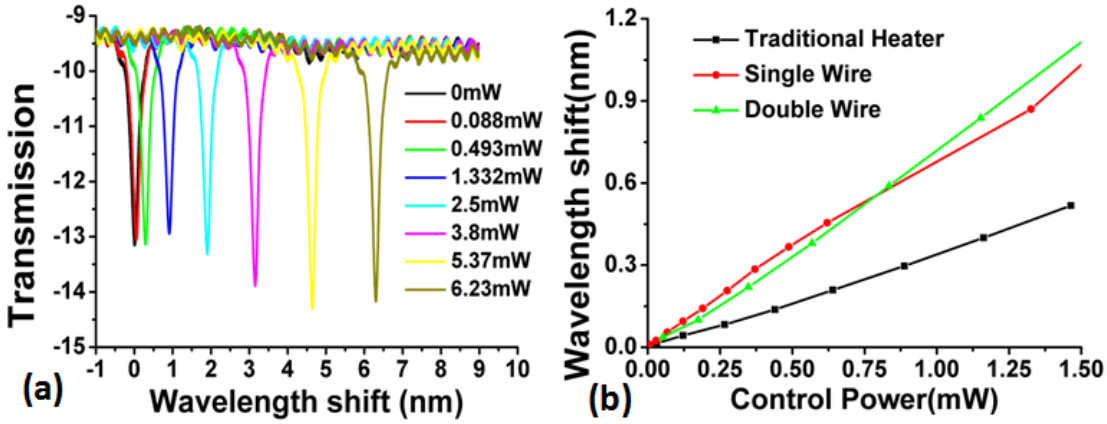

Fig.23 (a) Spectral response of 2.5micron radius micro-oven heater (b) Resonance wavelength change as function of heater power for traditional heater and micro-oven heaters with either a single-wire or double wire configuration [11].

PUBLICATIONS

1. Ali. W. Elshaari, Abdelsalam. A. Aboketaf, and Stefan F. Preble, “Controlled Storage of Light in Silicon Cavities,” Optics Express,18, 3014-3022 (2010).
2. Donald Adams, Greg Madejski, Stefan F. Preble, “High-Q Shallow Etch Silicon Micro Resonators for Optical Delay,” IEEE Photonics 2011, Arlington, Virginia, October 2011.
3. S. F. Preble, L. Cao, A. Elshaari, A. Aboketaf, D. Adams, “Single Photon Adiabatic Wavelength Conversion,” Appl. Phys. Letters 101, 171110 (2012).
4. L. Cao, A. Elshaari, A. Aboketaf, S. Preble, “Single Photon Adiabatic Wavelength Conversion,” Frontiers in Optics, FTu4D.5, Rochester, New York, October 2012.
5. S. Preble, “Silicon Photonic Quantum Optical Devices,” SPIE 2013 Optics+Optoelectronics , Prague, 8773-6, April 2013.
6. E. E. Hach III, A. W. Elshaari, S. F. Preble, "Fully quantum-mechanical dynamic analysis of single-photon transport in a single-mode waveguide coupled to a traveling-wave resonator," Physical Review A 82, 063839 (2010).
7. S. Preble, E. Hach, A. Elshaari, “Multi-photon interactions in travelling wave resonators,” SPIE Defense, Security and Sensing, Proceedings of SPIE Volume 8749, 8749-26, Baltimore, May 2013.
8. E. E. Hach III, S. F. Preble, A. Elshaari, P. Alsing, M. Fanto, “Robust, scalable Hong-Ou-Mandel manifolds in quantum optical ring resonators,” In Preparation for Submission
9. A. Aboketaf, L. Cao, S. Preble, P. Ampadu, “Robust Phase-Shift-Keying Silicon Photonic Modulator,” Frontiers in Optics, FTu2A.3, Rochester, New York, October 2012.
10. D. B. Adams, A. A. Aboketaf, S. F. Preble, "Robust phase-shift-keying Silicon photonic modulator," Optics Express 20, 17440 (2012).
11. L. Cao, A. A. Aboketaf, S. Preble, “CMOS compatible micro-oven heater for efficient thermal control of silicon photonics devices,” Optics Communications 35, 66 (2013).
12. L. Cao, A. Aboketaf, S. Preble, “Efficient Thermal Control of CMOS Compatible Silicon Photonic Devices using a Micro-Oven,” Frontiers in Optics, FTu2A.4, Rochester, New York, October 2012.
13. L. Cao, A. Aboketaf, K. Narayanan, A. Elshaari, S. Kowsz, E. Freeman, S. McDermott, S. Preble, J. Bickford, N. Bambha, “Direct Observation of DC Kerr Electro-Optic Modulation using Silicon Nanocrystals,” Frontiers in Optics, FTu1A.5, Rochester, New York, October 2012.
14. J. Bickford, N. Bambha, S. Preble, “CMOS Compatible Modulation of 1.5-micron Light using Silicon Nanocrystals,” 2012 IEEE Avionics, Fiber Optics and Photonics Conference (AVFOP 2012), ThB3, Cocoa Beach, Florida, September 2012.
15. Ali Wanis Elshaari, “Photon Manipulation in Silicon Nanophotonic Circuits,” Ph.D. Dissertation, Rochester Institute of Technology, Microsystems Engineering, October 2011.

The following is the publication list in chronological order, including publications that are in preparation:

- Ali. W. Elshaari, Abdelsalam. A. Aboketaf, and Stefan F. Preble, “Controlled Storage of Light in Silicon Cavities,” Optics Express,18, 3014-3022 (2010).
- E. E. Hach III, A. W. Elshaari, S. F. Preble, "Fully quantum-mechanical dynamic analysis of single-photon transport in a single-mode waveguide coupled to a traveling-wave resonator," Physical Review A 82, 063839 (2010).
- Donald Adams, Greg Madejski, Stefan F. Preble, “High-Q Shallow Etch Silicon Micro Resonators for Optical Delay,” IEEE Photonics 2011, Arlington, Virginia, October 2011.
- Ali Wanis Elshaari, “Photon Manipulation in Silicon Nanophotonic Circuits,” Ph.D. Dissertation, Rochester Institute of Technology, Microsystems Engineering, October 2011.
- D. B. Adams, A. A. Aboketaf, S. F. Preble, "Robust phase-shift-keying Silicon photonic modulator," Optics Express 20, 17440 (2012).

- J. Bickford, N. Bambha, S. Preble, "CMOS Compatible Modulation of 1.5-micron Light using Silicon Nanocrystals," 2012 IEEE Avionics, Fiber Optics and Photonics Conference (AVFOP 2012), ThB3, Cocoa Beach, Florida, September 2012.
- S. F. Preble, L. Cao, A. Elshaari, A. Aboketaf, D. Adams, "Single Photon Adiabatic Wavelength Conversion," Appl. Phys. Letters 101, 171110 (2012).
- L. Cao, A. Elshaari, A. Aboketaf, S. Preble, "Single Photon Adiabatic Wavelength Conversion," Frontiers in Optics, FTu4D.5, Rochester, New York, October 2012.
- A. Aboketaf, L. Cao, S. Preble, P. Ampadu, "Robust Phase-Shift-Keying Silicon Photonic Modulator," Frontiers in Optics, FTu2A.3, Rochester, New York, October 2012.
- L. Cao, A. Aboketaf, K. Narayanan, A. Elshaari, S. Kowsz, E. Freeman, S. McDermott, S. Preble, J. Bickford, N. Bambha, "Direct Observation of DC Kerr Electro-Optic Modulation using Silicon Nanocrystals," Frontiers in Optics, FTu1A.5, Rochester, New York, October 2012.
- L. Cao, A. Aboketaf, S. Preble, "Efficient Thermal Control of CMOS Compatible Silicon Photonic Devices using a Micro-Oven," Frontiers in Optics, FTu2A.4, Rochester, New York, October 2012.
- S. Preble, "Silicon Photonic Quantum Optical Devices," SPIE 2013 Optics+Optoelectronics , Prague, 8773-6, April 2013.
- S. Preble, E. Hach, A. Elshaari, "Multi-photon interactions in travelling wave resonators," SPIE Defense, Security and Sensing, Proceedings of SPIE Volume 8749, 8749-26, Baltimore, May 2013.
- L. Cao, A. A. Aboketaf, S. Preble, "CMOS compatible micro-oven heater for efficient thermal control of silicon photonics devices," Optics Communications 35, 66 (2013).
- E. E. Hach III, S. F. Preble, A. Elshaari, P. Alsing, M. Fanto, "Robust, scalable Hong-Ou-Mandel manifolds in quantum optical ring resonators," In Preparation for Submission
- L. Cao, A. A. Aboketaf, D. B. Adams, S. F. Preble, "Electro-optic tunable delay," In preparation
- A. A. Aboketaf, L. Cao, D. B. Adams, S. F. Preble, "Robust PSK Electro-Optic Modulator with Integrated Differential Detection," In Preparation
- A. A. Aboketaf, L. Cao, S. F. Preble, "Amorphous Silicon Integrated Low-Voltage Lithium Niobate Electro-Optic Modulator," In Preparation

PERSONNEL SUPPORTED

The following personnel have been supported by the YIP award:

- **Abdelsalam Aboketaf** : Ph.D. Candidate; Expected Graduation December 2013
- **Dr. Donald Adams** : Postdoctoral Research Associate (Sept. 2010 – December 2012); Now at Cisco working on Silicon Photonic interconnects (formerly LightWire, Inc.)
- **Liang Cao** : Ph.D. Candidate; Expected Graduation December 2013
- **Dr. Ali Elshaari** : Former Ph.D. Student Graduated October 2011 ; Now a Professor at Benghazi University, Libya
- **Dr. Edwin Hach** : Research Scientist and Visiting Faculty Research Program fellowship at AFRL Rome under Dr. Paul Alsing and Michael Fanto (Summer 2012 & 2013); Now a Lecturer in the Physics Department at RIT
- **Juni Khisha** : M.S. student in Electrical and Microelectronic Engineering; Expected Graduation December 2013
- **Professor Stefan Preble** : Received tenure and promoted to Associate Professor at RIT as of April 2013